

# Mesoscale surface deflagration modeling of metalized solid propellants

Hong-Suk Choi and Jack J. Yoh

Department of Aerospace Engineering, Seoul National University

1 Gwanakro, Gwanakgu, Seoul 08826, South Korea

## Abstract

This study investigates mesoscale deflagration, a flame that develops on the surface of a metalized solid propellant. Convection and diffusion transport energy to the nearby material and are treated differently depending on the corresponding time scale. Convective and diffusive combustion are represented using the Arrhenius law, and the temporal and spatial domains are discretized using the third order Runge-Kutta method and Essentially Non-Oscillatory (ENO) schemes. The level-set function that describes the deforming interface keeps track of the contact between two materials. While conduction influences the heat transfer in the reaction zone, the intense compression wave in the convection-dominant region ignites the unreacted particles. The slow flame, which includes conductive heat transfer, is specifically treated separately from convective transfer using a large time step technique. For given values of pre-exponential factor and activation energy, convective burning is shown to be faster than the reference burn rate, whereas diffusive burning is shown to be slower because pressure does not trigger the ignition of the reactive particles. Work is currently being done to simulate the experimental burn rate by incorporating the stress field calculation related to grain interactions and accounting for all structural influences on the resulting thermo-chemical processes.

## 1 Introduction

Aerospace engineers concentrate on fuel efficiency since the launch vehicle is intended to be lighter overall, and environmental issues are also significant because traditional fuels produce pollutants. The engineers, therefore, decide to supplement a significant amount of metal particles to the base solid fuels because metal has a high energy density and is not environmentally hazardous. However, it is challenging to fully comprehend the sophisticated microscale reaction mechanism, because the behavior of metalized solid fuels varies significantly with respect to particle size. As a result, there is a lot of interest in the rocket propellant community about research on the chemical interactions between metal particles and solids exposed to gas environments.

Three distinct zones, such as the solid region, the melt layer, and the outflow region, might be identified when the solid fuel is ignited, covering the entire process from the unreacted solid state through the production of exhaust gases. The “solid region” refers to the metal particles with graphite and Viton that have not yet reacted. The metal begins to react in the “melt layer” after the solid has reached its

maximum temperature. Due to the high pressure that is created on the burning surface, a reactive gaseous flame is forced from the melt layer and into the “outflow region”. These three regions are demonstrated for the combustion of aluminum [1]. When the solid propellant burns with metal components, three separate types of flames are produced: the primary premixed flame, the primary diffusion flame, and the final diffusion flame. The combustion mechanism of the solid propellant in the mesoscale is highlighted, and this research explains the flame structure [2].

The outflow region where the complicated turbulent gas may be seen has been the main topic of similar studies [2,3]. It is essential to comprehend the melt layer's temperature dependence and metal particle reaction mechanism. It is predicted how compressible pressure from energetic material causes the after-burning of Al particles on the microscale [4]. This research is significant due to its size even though it didn't directly address the melt layer. This paper may be pursued with the goal of demonstrating the mesoscale burning of metal particles. This research aims to simulate mesoscale burning and examine the chemical and mechanical properties of a solid fuel that has undergone heterogeneous metallization.

In this research, we model mesoscale burning and investigate the chemical and mechanical aspects of a heterogeneously metalized solid fuel. Here, a numerical domain was used to model the mesoscale combustion of metalized solid propellant. Zirconium Potassium Perchlorate (ZPP), which is utilized as a solid fuel, is composed of 52wt% zirconium (Zr), 42wt% potassium chloride (KClO<sub>4</sub>), 5wt% Viton B, and 1wt% graphite. The particles are Zr with KClO<sub>4</sub>, and the binder is a combination of graphite and Viton B. In surface burning, the time scale used to represent the temperature variation during convective and diffusive burning is different.

## 2 Methodology

### 2.1 Governing equation

The 2-D Euler equation is used to simulate the mesoscale deflagration on the surface of a metalized solid; the Euler equation is defined below, along with its governing equation and each matrix part.

$$\frac{\partial U}{\partial t} + \frac{\partial E}{\partial x} + \frac{\partial F}{\partial y} = S(U) \quad (1)$$

$$U = \begin{bmatrix} \rho \\ \rho u_x \\ \rho u_y \\ \rho E \\ \rho \lambda \end{bmatrix}, \quad E = \begin{bmatrix} \rho u_x \\ \rho u_x^2 + P \\ \rho u_x u_y \\ u_x(\rho E + P) \\ \rho \lambda u_x \end{bmatrix}, \quad F = \begin{bmatrix} \rho u_y \\ \rho u_x u_y \\ \rho u_y^2 + P \\ u_y(\rho E + P) \\ \rho \lambda u_y \end{bmatrix}, \quad S = \begin{bmatrix} 0 \\ 0 \\ 0 \\ \rho Q \dot{\lambda} \\ \rho \dot{\lambda} \end{bmatrix} \quad (2)$$

U matrix consists of conservation variables, while E and F are the flux matrix of U in the X and Y direction. The conservative variables  $\rho$ ,  $u_x$ ,  $u_y$ ,  $E$ , and  $\lambda$  denote the density, x- and y-direction velocities, total energy, and reaction rate of ZPP, respectively. Here, the pressure is represented by P, while the heat of reaction is given by Q.

### 2.2 Numerical approach

The ENO scheme is used for two-dimensional spatial discretization, while the third-order Runge-Kutta method is employed for temporal discretization [3].

The pressure of reacted hot gas and unreacted particles is calculated using the Equation of State (EOS). Tait EOS is used for particles, whereas Nobel-Abel EOS is used for exhaust gas; each equation is expressed as follows [5].

$$P_u = B \left( \left( \frac{\rho}{\rho_0} \right)^N - 1 \right) + A \quad (3)$$

$$P_r = \frac{(\gamma-1)e}{v-b} \quad (4)$$

B, A, and N in Eqn. (3) are coefficients of Tait EOS, and b in Eqn. (4) is the co-volume of fluid for Nobel-Abel EOS. Unreacted particles and exhaust gas are mixed together during a chemical reaction, hence pressure at one grid is defined as the mass fraction combination of each calculated pressure.

According to pressure, the sound speed is described as follows.

$$c^2 = \frac{\partial P}{\partial \rho} \quad (5)$$

The EOS of each material is utilized to determine its sound speed. The mass fraction regulates the sound speed, just like it does for pressure. The global time step in this shock-capturing scheme relies on the eigenvalues containing the speed of sound as given below.

$$\Delta t = CFL \frac{\Delta x}{\max(u+c, u, u-c)} \quad (6)$$

The CFL condition affects the time step, and because the uniform grid length is 10<sup>-6</sup> m, the CFL number is then kept below 0.6. Eqn. (6) provides the velocity component's highest absolute value.

The Arrhenius rate law is used in the models of chemical reactions.

$$\frac{\partial \lambda}{\partial t} = A \exp \left( -\frac{E_a}{RT} \right) \quad (7)$$

A is the pre-exponential component, E<sub>a</sub> is the activation energy, and R is the universal gas constant. A value of exp(30.4)s<sup>-1</sup> and an E<sub>a</sub> value of 213 kJ/mol are determined using a calorimeter.

An original algorithm created in the lab is used in the internal code (C#) that is used to run this simulation.

## 2.3 Numerical domain

With 180,000 meshes (300 × 600), the numerical domain is 0.3 mm × 0.6 mm in the x and y dimensions. While the other boundaries have zero gradients, the bottom boundary has a wall condition.

In the ZPP model, the particle is represented by a mixture of Zr and KClO<sub>4</sub>, while graphite and Viton act as binders. The numerical domain contains 80 spherical shape particles with an average diameter of 48 μm, which are placed at random across the domain. Since the reaction of ZPP begins around 1400 K in the 0-D simulation, the 20% region of the upper boundary is heated from an initial temperature of 300 K to 1300 K.

## 2.4 Interface tracking technique

The interface between the materials should be clearly specified when more than two materials interact with one another. The level-set function, φ, which is determined using Euler's conservation equation to define the displacement from the node to the closest boundary is given below [6].

$$\frac{\partial \phi}{\partial t} + \frac{\partial(\phi u_x)}{\partial x} + \frac{\partial(\phi u_y)}{\partial y} = 0 \quad (8)$$

Depending on the kind of interface between the two materials, the level-set function's sign is determined. First, all material boundaries are represented as zero level-set. The node is thought to be inside the material for  $\varphi < 0$  and outside the material for  $\varphi > 0$ . Therefore, each material has a different level-set function, which depends on the material and the displacement to the boundary. This suggests that the Euler conservation equation must be performed for both of them when the level-set function is specified in the code. The diagram in Fig. 1 depicts the level set function's schematic for defining the boundary of two materials. The maximum absolute value of the level-set function is set to 6 times the grid size in order to focus on the near nodes of the interface.

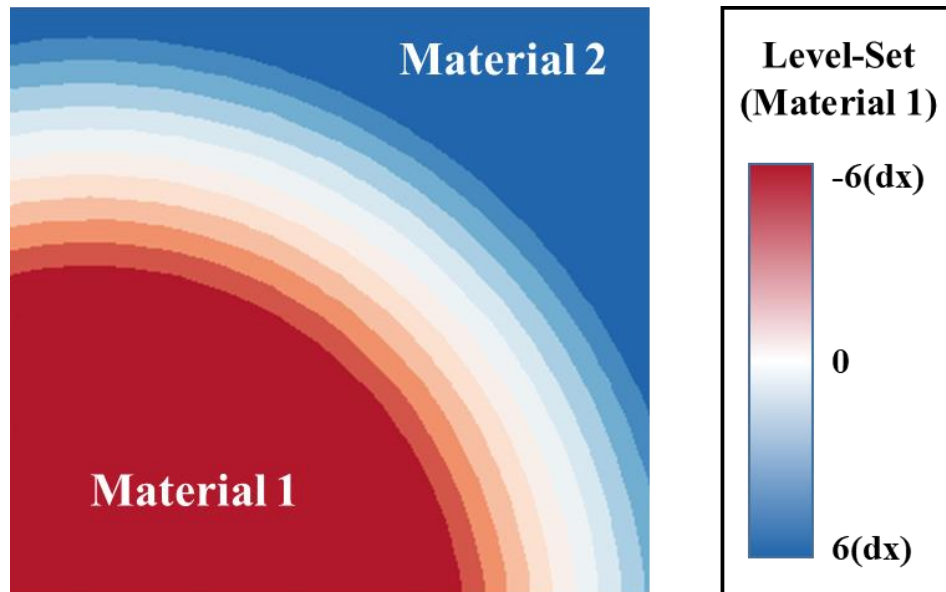


Figure 1: Definition of the level-set function illustrated schematically

### 3 Results

The temperature and pressure contour for the convective burning is shown in Fig. 2. The highest pressure point is varied for the initial distribution because the particles were generated at random in the domain. Meanwhile, the maximum pressure value remained at 150 MPa, whereas the burning surface pressure persisted at around 50 MPa. It was found that the temperature inside the material slowly increased to 1400 K after the granules were heated to 1300 K, and then rapidly increased to its maximum when the temperature exceeded 1400 K. The fast combustion in Fig. 2 demonstrated the high-speed deflagration via this growing pattern. Thus, it was possible to see the by-products that this high pressure had forced from the melt layer into the outflow region.

In addition to convection dominating fast combustion, diffusion dominating slow combustion was considered as well. Temperature aspects during diffusive burning are depicted in Fig. 3. In contrast to slow combustion, where the maximum temperature is restricted to 3900 K, convective burning can produce hot gas products with a maximum temperature of up to 5500 K. Because of the intricacy of the hydraulic interaction between the products and reactants, the maximum temperature is higher for convective burning. Additionally, as seen in Fig. 3, the particles react and release their heat through diffusion. Whereas the fast deflagration totally burns all of the particles in three microseconds, this procedure is completed in forty seconds. The reaction temperature is roughly 4700 K when the particle reaction is simulated in a 0-D state with the same activation energy and pre-exponential factor. This temperature represents the average of two results. The temperature measurements appear to be acceptable when taking into account pressure interaction and conduction.

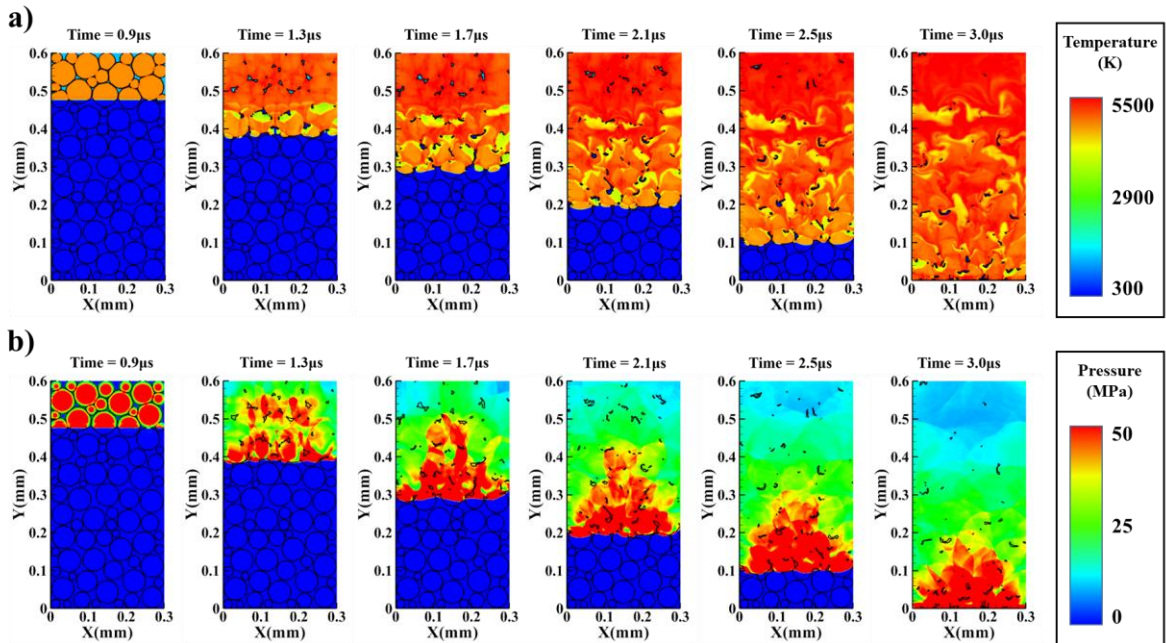


Figure 2: The varying a) temperature and b) pressure during convective burning

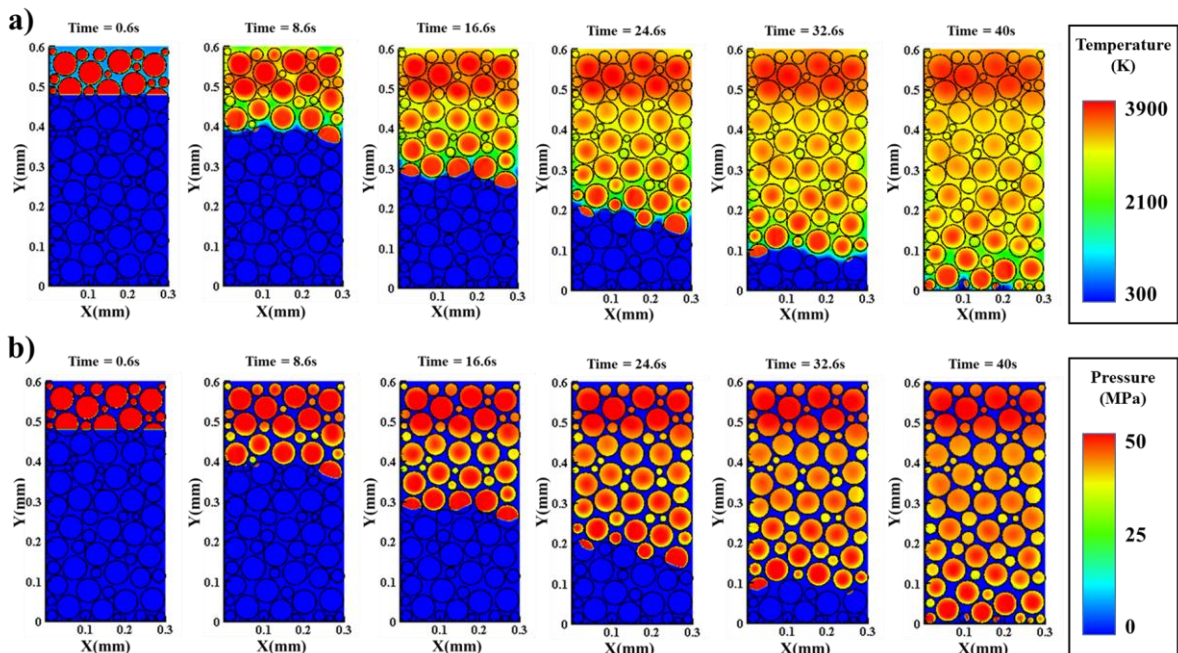


Figure 3: The varying a) temperature and b) pressure during diffusive burning

Equation (6) demonstrates that the time step is influenced by the grid length, sound speed, and velocity. The time step in convective burning is therefore in the nanosecond scale. Contrarily, in diffusive burning, convection was disregarded; hence, the CFL condition had no influence on the simulation's time step. Table 1 displays the determined burn rate and time scale for each simulation.

Table 1: Surface burning simulations' burn rate and time scale

Simulation	Burn rate (mm/s)	Time scale (s)
Fast deflagration	240,000	$10^{-9}\sim 10^{-8}$
Slow deflagration	50~170	$10^{-6}\sim 10^{-5}$
Diffusive burning	0.015	$10^{-2}\sim 10^{-1}$

It has been noted that the burning rate of ZPP is approximately 50-170 mm/s when the operating pressure is between 10 to 100 MPa [3]. Therefore, the 0.6 mm of ZPP should react entirely in 3–10 ms. The theoretical burn rate is around the mean value of two simulations that were run. As a result, after the time step issue is resolved, the activation energy and pre-exponential factor must be adapted to experimental values in order to validate the combustion simulation.

## 4 Conclusion

In this study, mesoscale surface combustion modeling of metalized solid fuel was applied. The formation of exhaust products, including solid byproducts and gas, is explored. A theoretical rate law was utilized to evaluate the activation of metalized solid propellant in the melt layer. Analytical illustrations are given for the physical and chemical interactions between the reactive particles and the exhaust gas on the burning surface. It is necessary to reduce the approximation and use experimental data for the chemical reaction to verify the simulation results with the expected burn rate, though. Furthermore, the conservation equation for internal stress must be utilized because the grains should maintain their shape after the shock wave from the reaction impacts them. Future research has proposed to apply the revised Euler equation that includes the internal stress term for the conservation variable with conduction calculation. It can make the heat flux be governed by diffusion in the solid region and convection in the outflow region. The melt layer is the target region of interest where the underlying process of surface interaction between unreacted particles and exhausting gases can be discovered.

## References

- [1] Sippel TR, Son SF, Groven LJ, Zhang S, Dreizin EL. (2015). Exploring mechanisms for agglomerate reduction in composite solid propellants with polyethylene inclusion modified aluminum. *Combustion and Flame*. 162: 846-854.
- [2] Beckstead MW, Derr RL, Price CF. (1970). A model of composite solid-propellant combustion based on multiple flames. *AIAA J*. 8: 2200-2207
- [3] Choi SH, Kim BH, Han SY, Yoh JJ. (2020). Multiscale modeling of transient in the shock-induced detonation of heterogeneous energetic solid fuels. *Combustion and Flame*. 221: 401-415.
- [4] Kim BH, Choi SH, Yoh JJ. (2019). Modeling the shock-induced multiple reactions in a random bed of metallic granules in an energetic material. *Combustion and Flame*. 210: 54-70.
- [5] Chiapolino A, Saurel R. (2018). Extended Noble–Abel Stiffened-Gas Equation of State for Sub- and-Supercritical Liquid-Gas Systems Far from the Critical Point. *Fluids*. 3: 48
- [6] Kim KH, Yoh JJ. (2008). Shock compression of condensed matter using multimaterial reactive ghost fluid method. *Journal of Mathematical Physics*. 49: 043511